


Review

Optically Tunable Magnetoresistance Effect: From Mechanism to Novel Device Application

Pan Liu ¹, Xiaoyang Lin ^{1,2,*} , Yong Xu ^{1,3}, Boyu Zhang ¹, Zhizhong Si ¹, Kaihua Cao ¹, Jiaqi Wei ¹ and Weisheng Zhao ^{1,2,*}

- ¹ Fert Beijing Research Institute, School of Electrical and Information Engineering, Big Data and Brain Computing Center (BDBC), Beihang University, Beijing 100191, China; liupan@buaa.edu.cn (P.L.); yong.xu@univ-lorraine.fr (Y.X.); boyu.zhang@buaa.edu.cn (B.Z.); szz931220@buaa.edu.cn (Z.S.); kaihua.cao@buaa.edu.cn (K.C.); weijiaqi@buaa.edu.cn (J.W.)
- ² Beihang-Geortek Joint Microelectronics Institute, Qingdao Research Institute, Beihang University, Qingdao 266000, China
- ³ Institut Jean Lamour, CNRS UMR 7198, Université de Lorraine, 54506 Vandœuvre-lès-Nancy, France
- * Correspondence: XYLin@buaa.edu.cn (X.L.); weisheng.zhao@buaa.edu.cn (W.Z.); Tel.: +86-108-233-9374 (W.Z.)

Received: 19 November 2017; Accepted: 16 December 2017; Published: 28 December 2017

Abstract: The magnetoresistance effect in sandwiched structure describes the appreciable magnetoresistance effect of a device with a stacking of two ferromagnetic layers separated by a non-magnetic layer (i.e., a sandwiched structure). The development of this effect has led to the revolution of memory applications during the past decades. In this review, we revisited the magnetoresistance effect and the interlayer exchange coupling (IEC) effect in magnetic sandwiched structures with a spacer layer of non-magnetic metal, semiconductor or organic thin film. We then discussed the optical modulation of this effect via different methods. Finally, we discuss various applications of these effects and present a perspective to realize ultralow-power, high-speed data writing and inter-chip connection based on this tunable magnetoresistance effect.

Keywords: spintronics; magnetoresistance effect; optically tunable; interlayer exchange coupling; data storage

1. Introduction

The appreciable magnetoresistance (MR) effect known as giant magnetoresistance (GMR) and tunneling magnetoresistance (TMR) appears in an artificial, nano-scale, sandwiched structure consisting of two ferromagnetic (FM) layers separated by a nonmagnetic spacer (Figure 1a). Its successful application has completely revolutionized the information industry and changed our daily life [1–3]. The underlying process of these MR effects is a switch of the relative magnetization arrangement, between an antiparallel (AP) arrangement and parallel (P) arrangement, during a sweep of the magnetic field. Such a magnetization switch induces a large change in electrical resistivity of the multilayers. The change is usually several orders of magnitude larger than the anisotropic magnetoresistance (AMR) effect [4]. The discovery of these appreciable MR effects has paved a way for transforming weak magnetic information into a large electrical signal, leading to numerous impactful applications. Representatively, the GMR- and TMR-reading head in a hard-disk drive (HDD) has boosted the computer storage density and capacity, which promoted the era of big data (Figure 1b) [2,5]. Additional design and optimization of the GMR/TMR sensors have further enabled applications of position and/or speed sensing [6,7], and even biological probing [8]. Moreover, the emerging nonvolatile magnetic memory (MRAM) based on the TMR effect has been widely considered as a competitive choice for next generation universal memory [2]. The integration of these

nonvolatile memory devices with complementary metal oxide semiconductor (CMOS) devices has been successfully applied for high-performance logic circuits [9]. Besides these direct applications of the GMR/TMR effect on sensing, data storage and processing, breakthroughs in the optical tuning of these effects further promise ultra-fast, high-volume data transmission solutions, which meet the ever-growing speed and bandwidth demands of inter-chip communication.

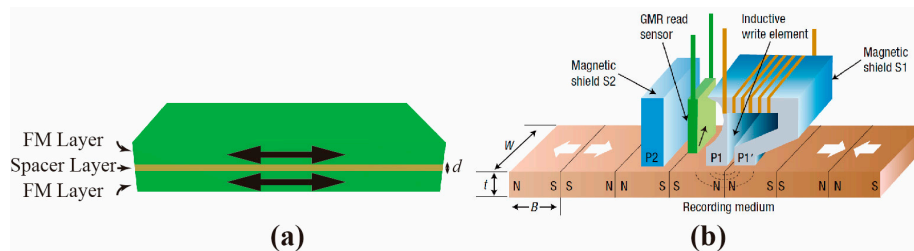


Figure 1. (a) Schematic of a GMR device with a FM layer/spacer layer/FM layer stacking. The thickness of the spacer layer is labeled as d ; (b) GMR read-head for hard drive [2]. Reproduced with permission from [2].

In the following sections, firstly we review the GMR/TMR effect and the IEC effect in different material systems, concurrently we discuss the related basic and forefront key research issues. Then we revisit the development and principles of the optical manipulation of the MR effect. Such manipulation can be realized via different methods, including switching the relative magnetic alignment via the all optical switching (AOS) of the magnetic layer or via tuning the IEC effect; or otherwise modulating the electronic transport of the optical responsive spacer layer. The final section is devoted to the abundant applications of those effects, including data storage and sensing. At the end we present a perspective for applying the optical tunable MR to realize ultra-low-power optical data writing and high-speed, inter-chip connection.

2. Magnetoresistance and Interlayer Exchange Coupling Effect

2.1. GMR/TMR Effect

The GMR and TMR effects originally describe the appreciable resistance change, during a sweep of applied magnetic field, of a magnetic sandwiched structure with a spacer layer of nonmagnetic metal or insulator, respectively. Here the magnetic field serves as a tool to switch the relative magnetization of magnetic layers. The system would exhibit relatively high resistance in antiparallel alignment, with low resistance in the parallel alignment.

In 1988, the GMR effect was first discovered in antiferromagnetic (AFM) interlayer-exchange-coupled Fe/Cr multilayers by two research groups separately led by A. Fert and P. Grünberg [10,11]. The AFM IEC, which we will discuss later, guarantees that the adjacent layers will be at AP alignment in its natural state. This makes it possible for the applied magnetic field to force a contrastive P alignment [5]. However, these coupled systems show low sensitivity to the magnetic field due to an enhanced saturation field, which can be a huge flaw for practical applications. Researchers then developed non-exchange coupled structures in which two magnetic layers have different cohesive fields [12,13], called pseudo spin-valves, or where one of them is magnetically pinned by an additional pinning layer via the exchange bias effect, called a spin-valve [14,15]. The spin-valve structure has greatly contributed to the successful application of GMR [5]. Apart from different approaches for creating distinct magnetic alignments, a GMR device also has different device geometries. At the beginning, GMR was detected by electric current flowing in the film plane (CIP), and later research developed the “current perpendicular to plane (CPP)” geometry [16–18] that shows a relatively stronger effect [19]. The GMR effect rapidly found impactful applications in data storage, and attracted tremendous research interest.

The success of the GMR effect strongly incentivized research into the TMR effect. The very first report on TMR actually came before the discovery of GMR [20]. However, that experiment had been performed at low temperature and was hardly reproducible. The breakthrough of appreciable and reproducible TMR at room temperature (RT) was achieved when amorphous AlO_x was adopted as a tunneling barrier in the magnetic tunnel junction (MTJ) [21,22]. TMR as large as 81% at RT has been achieved in an optimized AlO_x -MTJ system [23]. With novel applications like MRAM still craving higher MR ratios, researchers continued exploring different materials and found by calculation [24], and then revealed by experiments, that MgO as barrier material could provide up to 1000% TMR ratio at 5 K [25–27]. MgO/CoFeB-based MTJ with perpendicular magnetic anisotropy (PMA), which presents higher switching energy efficiency and extra scalability, has become the mainstream for MRAM applications [28,29].

Along with the development of the magnetoresistance effect, the underlying physical mechanism has been better understood. The microscopic mechanism of the GMR and TMR effects is about electron transport dominated by spin-dependent scattering [30,31] or tunneling [20,24] respectively. As described by Mott's two-current model [32,33], electrons of spin-up or spin-down can be imagined to transmit through two independent channels. If the multilayer is in parallel arrangement, electrons with a spin direction the same as the magnetization direction will be less scattered (for GMR) or have higher tunneling probability (for TMR), resulting in low resistance. Conversely, electrons with a spin direction opposite to the magnetization direction will encounter a large resistance. Thus, the total resistance of the two channels in parallel connection will be relatively small, while if the multilayer is in an antiparallel arrangement, both channels will encounter a large resistance, hence leading to a large total resistance [2]. To realize such a spin-dependent interaction, electrons, which convey the spin information, should be able to maintain their spin momentum. This is why materials of spacer layer with a long mean-free-path (for CIP GMR), spin-diffusion-length (for CPP GMR) and small thickness (for both GMR and TMR) are necessary for an appreciable GMR/TMR effect. Values of these MR effects will depend on the spin-polarization of magnetic materials, the maintenance of spin momentum across spacer/barrier materials and the interfaces, and additional spin filtering effects induced by specific tunneling barriers [34]. As a result, well controls of the ferromagnetic materials, spacer/barrier materials and their interfaces, together with the emergent techniques of magnetic switching and MR effect modulation have been considered as key issues of spintronic research [1,35,36].

2.2. Interlayer Exchange Coupling Effect

The discovery and development of the GMR effect, which relies on the manipulation of the relative magnetic arrangement, has been intimately linked to the research achievement of the IEC effect [37–39]. IEC describes the magnetic interaction between two FM layers, mediated by a nanometer-thick spacer layer. IEC can be AFM or FM, depending on the spacer layer with specific thickness, which determines whether AP or P is the energy favorable state [40]. The IEC has been systematically established in numerous layered structures with different metallic spacer layers [41–44], as well as some semiconducting, insulating and organic molecular spacers e.g., Si [45–47], GaAs [48,49], MgO [50,51] and α -sexithiophene [52]. More interestingly, IEC strength is found to oscillate periodically between AFM and FM states, with varying thicknesses of metallic spacer layer [41–43,53].

The unusual phenomena of IEC has attracted a great deal of research interest in its mechanism. Microscopically, IEC is an indirect exchange interaction mediated by the electrons of the spacer layer. Pioneering theoretical researchers have tried to develop a unified theory for both metallic and insulating spacer layers, by introducing the concept of a complex Fermi surface [54,55]. A more recent and commonly accepted theory is that the oscillatory IEC is mediated by the quantum well states (QWS), which have been experimentally observed to occur in the spacer layer [40,56]. QWS describes the discrete electronic states formed by electron confinement, and those states evolve periodically with the well width [40,57,58]. The theoretical explanation of the IEC effect by QWS can be briefly interpreted as follows.

The IEC coupling strength J (value positive for AFM and negative for FM coupling, indicating the energy minimization principle) is determined by the energy difference between AFM and FM coupling states (E_{FM} and E_{AFM} represent the energy of the FM and FM coupling states, respectively) [40]:

$$2J = E_{FM} - E_{AFM} \quad (1)$$

The energy of electron gas in the spacer layer can be obtained by

$$E = \int_{-\infty}^{+\infty} \varepsilon D(\varepsilon) f(\varepsilon) d\varepsilon \quad (2)$$

where $D(\varepsilon)$ represents the density of states (DOS), and $f(\varepsilon)$ represents the distribution function [40,55]. Due to the splitting of the bands in the magnetic materials, the electrons in the spacer layer with their spins opposite to the magnetization are strongly reflected at the interfaces between the FM layer and the spacer layer. Thus, when two magnetic layers are aligned parallel (direction ‘up’ in our example), as illustrated in Figure 2b, spin down electrons are strongly reflected at both interfaces, like being trapped in a well, which leads to their confinement. In contrast, such a quantum well situation cannot occur when the two magnetic layers are aligned antiparallel, as in Figure 2a, because either spin up or spin down electrons can always penetrate one of the two interfaces with little reflection. Therefore, the DOS of spin up electrons in the FM coupling state (D_{FM}) is strongly altered by confinement into nearly a set of delta functions at discrete energy levels, different from the continuous DOS of the AFM coupling state (D_{AFM}), as shown in Figure 2a,b. According to Equation (2), these different coupling states result in an inequity between E_{FM} and E_{AFM} . Such an energy difference ultimately determines the natural preference of one magnetization arrangement over another, which is manifested as the different types of IEC. Following this theory, the oscillatory behavior of IEC in certain material systems can be well understood. As the thickness of the spacer layer increases, the QWS energy levels shift downwards according to quantum mechanics, which generally decreases the E_{FM} . However, when a QW state crosses the Fermi level (E_F) from above, it adds to the integration term in Equation (2), meaning that E_{FM} increases sharply, which is when FM coupling turns out to be unfavorable [40]. Therefore, changes of the E_{AFM} contribute to the alteration of two types of IEC. (More details of this mechanism can be found in Reference [5]).

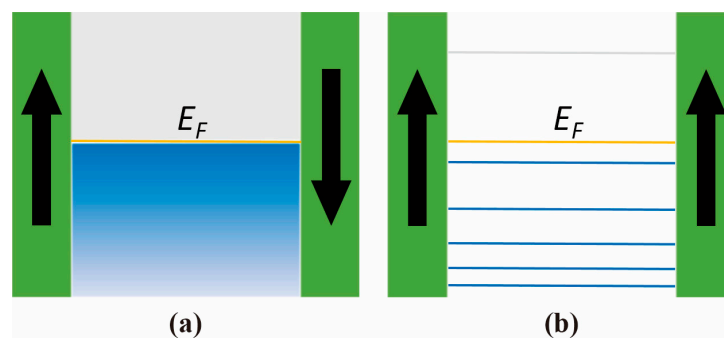


Figure 2. Electron distribution schema of the (a) AFM coupling and (b) FM coupling state. At the ground state, electrons occupy only those states below the Fermi level (E_F) (occupied states are colored blue, unoccupied colored gray).

Based on the mechanism of the IEC effect, it is possible to design magnetically-coupled multilayers with negligible influence to other adjacent layers (that is, synthetic anti-ferromagnet (SyAF), see references [36,59,60]). The SyAF technique has already contributed to the booming of the HDD market and the development of MRAM. Besides, the IEC effect also implies a tricky strategy to realize magnetic switching by switching the coupling type [52,61–65].

2.3. MR in Different Material System

Traditional MR structures usually consist of two FM metal layers separated by a nonmagnetic metal spacer (for GMR) or a metal-oxide barrier (for TMR). As indicated by the mechanism of the GMR/TMR effect, the choice of the spacer can affect the GMR/TMR effect by various critical aspects, including interface lattice match, spin polarization, spin-diffusion length, mean-free path, etc. The observation of GMR first succeeded in the molecular beam epitaxy (MBE)-grown, Fe/Cr/Fe, AFM-coupled, nanometer-thick multilayers with well-defined interfaces [10,11], and later systematically extended to various nonmagnetic spacer-based systems, including Fe/Cr, Co/Ru, etc. [41–44]. Among them Co/Cu, whose well-matched crystal structures minimize interface defects and thus consequential spin-independent scattering, showing a strong MR and IEC effect, making it an archetypical GMR system [1,42,44]. As for TMR, despite some early observations regarding the Ge-based junction [20], strong TMR at RT was not achieved until the amorphous AlO_x barrier was adopted [21,22]. A further milestone has been the theoretical prediction and successful observation of a high TMR ratio in MgO-based systems, where the selective tunneling property of MgO with certain crystal orientations enhances spin polarization [24–26]. With the MgO-based junction prevailing in current TMR applications for its large TMR ratio, researchers continue searching for novel material systems [66–68], including the choice of capping materials [69–71], towards better device performance, such as larger TMR, a lower resistance area (RA), higher breakdown voltage and lower spin-torque switch current density [28,29].

Apart from traditional MR structures, tempted by relatively long spin diffusion length and the potential of electrical and optical modulation methods in semiconductors [1,72], plentiful attempts have been made to develop MR devices based on semiconductor spacers, including AlAs, GaAs, Si etc. [72–74]. Unlike all-metal systems, several key issues still remain to be tackled for semiconductor spacer-based heterostructures. These issues include the lattice mismatch and intermixing effect which result in poor interfaces between the FM metal and semiconductor, together with the impedance mismatch that makes the MR too weak to be detected [72,75,76]. Possessing the same advantage of long spin diffusion length as semiconductors, organic materials furthermore promise economic mass fabrication and flexible property manipulability from the material's perspective [77–80]. Various types of organic materials have been employed as a spacer material, with moderate MR ratios achieved, notably carbon nanotubes [81,82] and small organic molecules like sexithienyl (T₆) and 8-hydroxy-quinoline aluminium (Alq₃), etc. [83–86]. Additionally, the photosensitivity of certain organic materials allows the combination of the MR effect and photoresponse in a single device, as researchers recently proved using fluorinated copper phthalocyanine (F₁₆CuPc) and C₆₀ fullerene spacer-based devices [87,88]. A similar case lies in the poly(vinylidene fluoride) (PVDF)-based MTJ, which enables both magnetic and ferroelectric control of the device [89,90]. Besides exploring spacer or barrier materials, attempts have also been made to apply novel magnetic layer materials, for instance half-metals, which provide fully polarized electrons [91,92], or defect-induced magnetism (DIM) material [93,94], or materials with magnetization tunable by light [95–97], voltage [98,99], heat [100], etc. The introduction of these novel MR material systems, which either provide an improved MR ratio or permit additional methods of tuning MR, greatly adds to the theoretical and applicational richness of the MR effects.

3. Optically Tunable MR Effect

Since the MR effect predominantly relies on the relative arrangement of the two magnetic layers, a key issue of its application is the ability to control the relative magnetic orientation [101]. Several approaches have been put forward: (1) The very intuitive magnetic field switching approach; (2) The electric current switching approaches using spin transfer torque (STT) [102–104] or spin orbit torque (SOT) mechanisms [105–107]; (3) Novel electric field, heat or strain-assisted approaches [108–111]. However, the operating speed of those approaches are ultimately constrained by the spin precession time [112]. Moreover, those electric approaches always have bottlenecks of

bandwidth and data loss issues for high-speed, inter-chip communication. Given that, for highly demanding novel device applications, optical approaches for high-speed MR modulation or even magnetic switching have been pushed to the frontier of research [35]. The realization of optically tunable magnetoresistance (OTMR) promises the integration of the ultra-fast, high-volume feature of optical information transmission with the non-volatility, high-density features of spintronics magnetic storage.

Intuitively there are different viable solutions for the optical approach: light can be applied either to the magnetic layer for a direct influence on magnetization [95–97,112]; or to the spacer layer, to tune the IEC, which would consequently affect the magnetic arrangement [61,64,65], or otherwise to tune the electric transport properties [87,88,113,114]. The material choice for the former could be the AOS magnetic materials, whose magnetization can be switched directly by light. The latter demands materials with electronic properties effectively tunable by light, such as VO₂ with a metal-insulator transition (MIT) feature, optically-sensitive semiconductor, and Phthalocyanine (Pc), etc. (Figure 3).

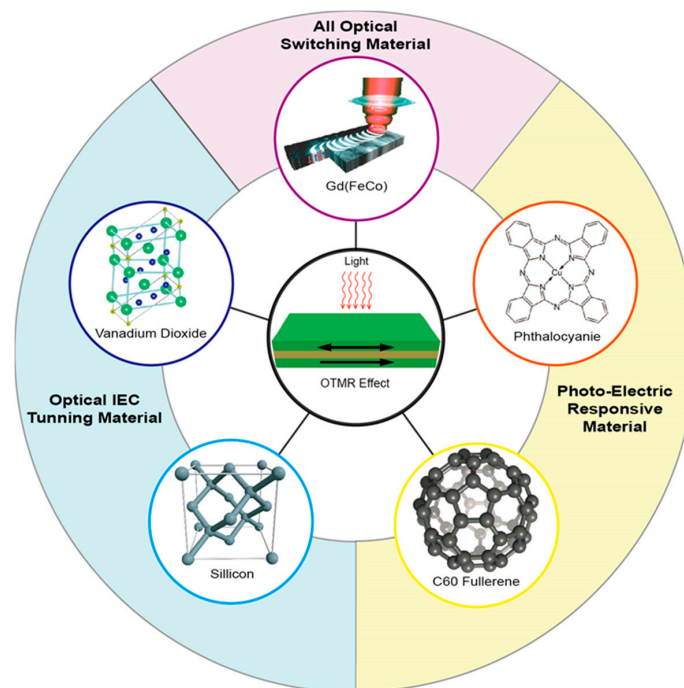


Figure 3. Examples of potential materials for the OTMR effect. Including AOS materials for the FM layer [95]; and phase-transition material VO₂, organic and inorganic photosensitive materials for the spacer. Reproduced with permission from [95].

3.1. All Optical Switching

Motivated by the demands of high-speed, large-volume storage applications, researchers have exploited using light instead of magnetic fields to manipulate magnetization in data recording materials. While laser has already been used as a heating source in the so-called heat-assisted magnetic recording (HAMR) to assist magnetic field-driven switching [115], early theoretical and experimental studies meanwhile confirmed light as an electro-magnetic wave can directly influence the magnetization [116]. Major breakthroughs of AOS, which means deterministic magnetic switching triggered purely by femtosecond laser pulse, have been achieved during the last decade. Two types of AOS have been observed experimentally, namely all optical helicity-dependent switching (AO-HDS) and all optical helicity-independent switching (AO-HIS), depending on whether the magnetic switching relies on the helicity of light. AO-HDS was once believed to be an effect limited to the rare earth-transition metal alloy [95]. More recently, general principles for designing and fabricating AOS material systems have

been put forward, broadening the AOS material choices to include synthetic ferrimagnetic multilayers and heterostructures, as well as RE-free pure ferromagnetic [Pt/Co], [Ni/Co] multilayers, etc. [96,117], transparent medium Cobalt-substituted yttrium iron garnet (YIG:Co) [118], and high-anisotropy FePt film which is a commonly used HAMR media [117]. The other type of AOS, the AO-HIS, has been discovered in GdFeCo alloy [119]. The magnetization of GdFeCo switches after each single pulse of femtosecond laser independent of the light helicity. The switching process is driven by the ultrafast heating with a signature of transient ferromagnetic states [120]. Apart from this direct switching by light, recent studies also found another switching mechanism for GdFeCo capped by thick metal layers, which contributes the switching to indirect hot electrons generated by light and propagating through the metal layers [121,122]. Despite intensive theoretical investigation dedicated to this, ambiguity still shadows the mechanism of the AO-HDS. Many fundamental questions remain to be answered, such as the role of the domain size [123], the role of optical spin transfer torque [124], the contribution of magnetic circular dichroism [125] and the role of the inverse Faraday effect [126].

Although the research into AOS is still in its early stage, people have already been attempting to bring it into application. Recently a pioneering demonstration of a GdFeCo-based AOS MTJ device was accomplished. Its free layer and pinned layer materials are GdFeCo and Co/Pd, respectively. The switching between parallel and antiparallel configurations was achieved by switching the GdFeCo using femtosecond laser pulse, although only a low MR ratio of 0.6% was achieved at RT (Figure 4) [112]. Moreover, in another newly reported experiment, a picosecond electric pulse of 9 ps was optically generated by a photoconductive switch. Such a picosecond electric pulse can induce ultrafast magnetic switching in GdFeCo toggles, which implies possible applications for ultrafast spintronic devices [127]. Further progress of this field will strongly rely on the development of on-chip photonics, emerging materials with lower requirement of the laser, and advanced device applications.

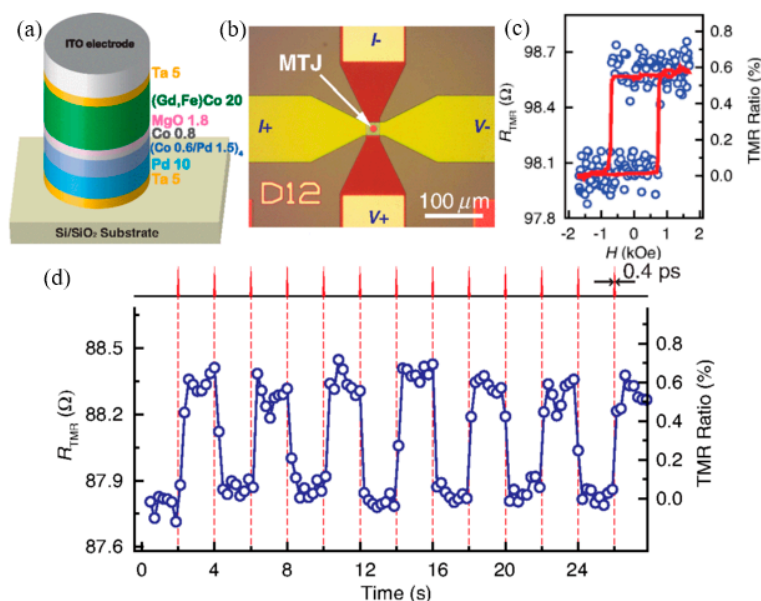


Figure 4. Device demonstration of AOS in an MTJ with subpicosecond single laser pulses without external magnetic field at RT. (a) Schematic of the MTJ structure used in the experiment; (b) Optical microscope image of a typical MTJ device with an indium tin oxide (ITO) electrode on the top for TMR measurement; (c) The $R_{\text{TMR}}(H)$ minor loop measured by sweeping a perpendicular magnetic field, which switches the Co/Pd layers (R and H represent resistance and magnetic field separately). The red line is the smoothing of the raw data (open circles); (d) R_{TMR} of the MTJ device measured during AOS by 0.4-ps single laser pulses at 0.5-Hz repetition rate. The changes of R_{TMR} in (c,d) have the same value of $\sim 0.6 \pm 0.05 \Omega$, indicating the GdFeCo layer has been completely switched. Reproduced with permission from [112].

3.2. Optical Tuning of IEC Effect

Manipulations of the GMR/TMR effect usually depend on the direct switching of magnetization in the FM layer, for example, via a magnetic field, a spin current or a laser pulse. However, the existence of coupling between neighboring FM layers implies the possibility of realizing the switching via a control of the IEC type. Since the IEC effect relies on the electronic properties of the spacer layer, in theory it could be effectively tuned by light in devices based on an optically sensitive spacer. Following the underlying QWS mechanism of IEC as stated earlier, we can understand from the energy's perspective the consequence that if the spacer layer is exposed to certain photon irradiation with sufficient fluence, owing to the different DOS, the electron gas in the AFM and FM coupling states will separately go through different absorption-transition behaviors, thus bringing about different light-induced energy changes. This could consequently change the relative magnitude between E_{AFM} and E_{FM} , which would induce switching between two states as a consequence.

Some experimental and theoretical studies have revealed its feasibility. Pioneering work has been carried out with semiconducting spacer-based systems. In 1993, a photon-induced IEC change from FM coupling to AFM coupling in Fe/(Fe-Si) superlattices at low temperature was reported [61,128], though with certain controversy [62,64]. Apart from optically-sensitive semiconductors, another notable material proposal is the VO₂, which features the MIT property [65]. Researchers performed first principle calculations of the IEC effect between Co-doped, TiO₂/VO₂-diluted magnetic semiconductor multilayers. Their results indicated that reversible switching from FM IEC to AFM IEC can be realized utilizing the temperature-induced MIT feature [65], which might be induced by light as well. Thanks to this progress in different material systems, device demonstration via optically-tuned IEC may be realized in the near future.

3.3. Optically Sensitive MR Effect

In some material systems, unlike the previous two cases, light illumination on the spacer does not necessarily provoke deterministic switching of the magnetic alignment, while the MR can still be effectively tuned due to the alteration of electronic transport properties [87,88,113,114]. Representatively, such effects are achieved in fluorinated copper phthalocyanine (F₁₆CuPc) and C₆₀ fullerene-based spin valve structures [87,88]. In the former system, photo-generated charge carriers in the spacer dominate the electric conductivity of the system [87]. Yet in the later, photon irradiation generates a photovoltage [88]. In both cases, the MR effect can be superimposed on the photoresponsive effects. Therefore, by cooperatively adjusting the light irradiation and the applied magnetic field, we can either obtain controllable multiple resistance states, or eliminate the base current of the MR effect [87,88], which can have abundant applications in high-density data storage and neuromorphic devices [129].

4. Application

4.1. Application of the GMR/TMR Effect

The rapid adoption of the GMR/TMR HDD head has long been regarded as a successful example of fundamental research advances quickly transforming into significant commercial applications. Thanks to the introduction of the GMR/TMR HDD head, we witnessed the capacity of HDD to grow by over thousands of times in two decades, intriguing a revolution in data-storage which constitutes the basis of this information era [2]. Besides, possessing unique high sensitivity and large response in such a small size, the GMR/TMR magnetic sensor can be specifically designed to fit in a vast range of application scenarios. For example, scalable down to sub- μm size, the TMR sensor permits very high spatial resolution, making it suitable for high-precision position, angle and motion sensing [19,130–132]. Also, the MR sensors are sensitive enough for detecting geomagnetic fields; meanwhile they can be integrated into integrated circuit (IC) chips, which makes them widely adopted for navigation, posture detection, etc. [19,130,133]. With the boom of the Internet of things (IoT), these sensing applications are

becoming ubiquitous, from daily life to industry management. Another promising field for GMR/TMR sensors consists in biosensing, where they are used to detect the surface binding reaction of certain biological molecules labeled with magnetic particles, enabling non-invasive, quick and inexpensive medical diagnosis [130,134–136]. Still, MR sensors can find broader niche applications, like detecting defect regions in metal parts, monitoring current density in IC chips, etc. [130,133,137].

Moreover, as the pillar of spintronics, the MR effect has the potential to play a major role in the beyond-Moore era [35]. One great dilemma of today's electronic industry is the ever-increasing power consumption brought on by growing computing demands, contradictory to the pursuit of portability and the compaction of products. TMR-based MRAM, which features certain key advantages including non-volatility, low-voltage operation, high-speed, and nearly infinite endurance, permits alleviating this issue [36,138]. Major chip fabricators have been targeting MRAM as embedded memory to substitute current volatile RAMs. With its scalability, MRAM also has the potential to be applied to large volume data storage [139,140]. Besides, a novel conceptual magnetic data-storage device named racetrack memory, which uses the TMR effect to read information stored in dynamic magnetic domains or skyrmions, is also under development [141,142].

Lastly, the development of GMR/TMR effects also benefits spintronics-based logic applications. The integration of MTJ-based memory with CMOS has been successfully applied for high-performance logic circuits [9]. Moreover, the development of GMR/TMR has boosted research advancements into magnetic and barrier materials, together with the control of the interfaces. Those achievements continue promoting various spintronics-based logic applications such as all-spin-logic, spin wave logic, etc., which highly rely on efficient spin-charge conversion and the modulation of spin propagation [143,144].

4.2. Application of OTMR Effect

The light-tunable MR effect indicates a novel path for combining photonics with magnetic technologies [112]. The first intriguing application consists of the data writing of magnetic memory. The optical writing of a novel AOS-material-based memory bit can be achieved with a single femtosecond laser pulse [95,121], requiring the switching energy prospectively to be much lower than the current electrical switching approaches [145]. Admittedly, before reaching a point of practical application, it still demands further research for AOS material systems with higher MR ratios, and efforts at the device engineering level to realize downscaled devices switchable by low-power laser. Different to the optically-switchable MR devices, which mainly provide higher speed and power-efficiency, the optically-sensitive MR devices feature other advantages. For example, stable multiple resistance states can be achieved in a single optically-sensitive MR device, which permits improved density for data storage applications, or otherwise can find its place in various novel neuromorphic applications. On the other hand, an optically-sensitive, zero-base-current MR device can function with significantly lower power-consumption [88].

As a perspective, once the on-chip laser technology matures, and a breakthrough of the high-MR AOS material systems arises, the optically-switchable MR will enable the integration of the ultra-fast, high-volume optic information transmission technology and the non-volatile, high-density spintronics magnetic storage technology, which would inaugurate a new vision of efficient data writing and inter-chip communication (Figure 5).

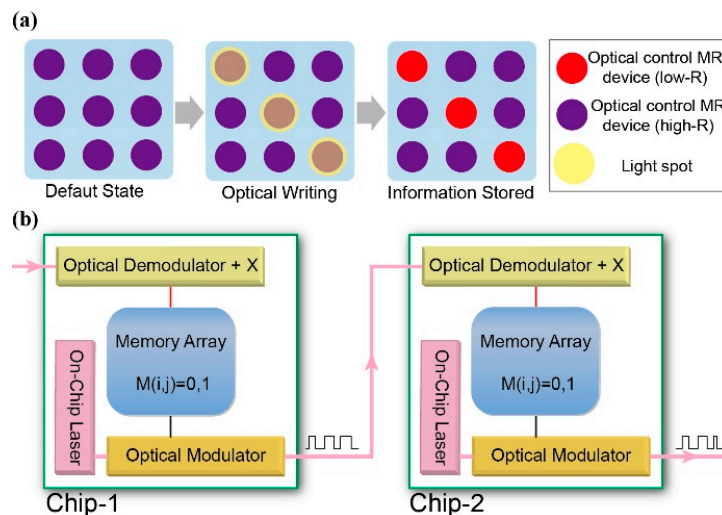


Figure 5. Schematic of the potential applications of the OTMR effect (a) Data writing in optical control MR chip. This chip, based on the OTMR devices array, can serve as a memory module in the following chips in (b); (b) Inter-chip optical communication. According to the data stored in the “Memory Array” on Chip-1, the laser beam from the “On-Chip Laser” can be modulated by the “Optical Modulator” to convey the information. Once another chip (“Chip-2”) receives the modulated laser beam from Chip-1, the “Optical Demodulator + X” unit will demodulate the beam and then write the “Memory Array” on Chip-2 in an optical writing way utilizing the laser-induced change of MR (the “X” may be a laser demultiplexer to perform selected data writing into specific memory unit).

5. Conclusions

The collision and blending of magnetics, electronics and nanotechnology have triggered the birth of spintronics, which is marked by the discovery of the GMR and TMR effect. These magnetoresistance effects and other emerging effects, with abundant applications in the information industry, have kept changing our daily life for several decades. In this paper, we have reviewed the development of GMR, TMR and other related effects, from their mechanism to novel device applications. We first revisited the discovery and mechanism of GMR, TMR and IEC effects within various material systems. We then reviewed the optically tunable MR effect by different approaches. Finally, we discussed the abundant applications of these MR effects and presented a perspective to realize efficient data writing and inter-chip communication.

Acknowledgments: This work was financially supported by National Natural Science Foundation of China (No. 61571023, No. 51602013, No. 61627813, No. 61504006), the International Collaboration 111 Project (No. B16001) and the Beijing Natural Science Foundation (No. 4162039).

Author Contributions: Pan Liu, Xiaoyang Lin contributed equally to this work. Pan Liu, Xiaoyang Lin and Weisheng Zhao conceived and designed the paper. Pan Liu, Xiaoyang Lin, Yong Xu, Boyu Zhang, Zhizhong Si, Kaihua Cao, Jiaqi Wei and Weisheng Zhao performed the discussion.

Conflicts of Interest: The authors declare no conflict of interest.

References

1. Fert, A. Nobel Lecture: Origin, development, and future of spintronics. *Rev. Mod. Phys.* **2008**, *80*, 1517–1530. [[CrossRef](#)]
2. Chappert, C.; Fert, A.; Van Dau, F.N. The emergence of spin electronics in data storage. *Nat. Mater.* **2007**, *6*, 813–823. [[CrossRef](#)] [[PubMed](#)]
3. Fullerton, E.E.; Schuller, I.K. The 2007 Nobel Prize in Physics: Magnetism and Transport at the Nanoscale. *ACS Nano* **2007**, *1*, 384–389. [[CrossRef](#)] [[PubMed](#)]

4. Rizal, C.; Moa, B.; Niraula, B. Ferromagnetic Multilayers: Magnetoresistance, Magnetic Anisotropy, and Beyond. *Magnetochemistry* **2016**, *2*, 22. [[CrossRef](#)]
5. Grünberg, P.; Bürgler, D.E. Metallic Multilayers: Discovery of Interlayer Exchange Coupling and GMR. In *Handbook of Spintronics*; Xu, Y., Awschalom, D.D., Nitta, J., Eds.; Springer: Dordrecht, The Netherlands, 2016; pp. 107–126. ISBN 978-94-007-6892-5.
6. Parkin, S.; Jiang, X.; Kaiser, C.; Panchula, A.; Roche, K.; Samant, M. Magnetically engineered spintronic sensors and memory. *Proc. IEEE* **2003**, *91*, 661–680. [[CrossRef](#)]
7. Daughton, J.M. GMR and SDT sensor applications. *IEEE Trans. Magn.* **2000**, *36*, 2773–2778. [[CrossRef](#)]
8. Osterfeld, S.J.; Wang, S. MagArray Biochips for Protein and DNA Detection with Magnetic Nanotags: Design, Experiment, and Signal-to-Noise Ratio. In *Microarrays*; Dill, K., Liu, R.H., Grodzinski, P., Eds.; Springer: New York, NY, USA, 2009; pp. 299–314. ISBN 978-0-387-72719-6.
9. Hanyu, T.; Endoh, T.; Suzuki, D.; Koike, H.; Ma, Y.; Onizawa, N.; Natsui, M.; Ikeda, S.; Ohno, H. Standby-Power-Free Integrated Circuits Using MTJ-Based VLSI Computing. *Proc. IEEE* **2016**, *104*, 1844–1863. [[CrossRef](#)]
10. Baibich, M.N.; Broto, J.M.; Fert, A.; Nguyen, V.D.F.; Petroff, F.; Etienne, P.; Creuzet, G.; Friederich, A.; Chazelas, J. Giant magnetoresistance of (001)Fe/(001)Cr magnetic superlattices. *Phys. Rev. Lett.* **1988**, *61*, 2472–2475. [[CrossRef](#)] [[PubMed](#)]
11. Binasch, G.; Grunberg, P.; Saurenbach, F.; Zinn, W. Enhanced magnetoresistance in layered magnetic structures with antiferromagnetic interlayer exchange. *Phys. Rev. B* **1989**, *39*, 4828–4830. [[CrossRef](#)]
12. Speriosu, V.S.; Dieny, B.; Humbert, P.; Gurney, B.A.; Lefakis, H. Nonoscillatory magnetoresistance in Co/Cu/Co layered structures with oscillatory coupling. *Phys. Rev. B* **1991**, *44*, 5358–5361. [[CrossRef](#)]
13. Dupas, C.; Beauvillain, P.; Chappert, C.; Renard, J.P.; Trigui, F.; Veillet, P.; Velu, E.; Renard, D. Very large magnetoresistance effects induced by antiparallel magnetization in two ultrathin cobalt films. *J. Appl. Phys.* **1990**, *67*, 5680–5682. [[CrossRef](#)]
14. Dieny, B.; Speriosu, V.S.; Parkin, S.S.; Gurney, B.A.; Wilhoit, D.R.; Mauri, D. Giant magnetoresistive in soft ferromagnetic multilayers. *Phys. Rev. B* **1991**, *43*, 1297–1300. [[CrossRef](#)]
15. Dieny, B. Giant magnetoresistance in spin-valve multilayers. *J. Magn. Magn. Mater.* **1994**, *136*, 335–359. [[CrossRef](#)]
16. Zhang, S.; Levy, P.M. Conductivity perpendicular to the plane of multilayered structures. *J. Appl. Phys.* **1991**, *69*, 4786–4788. [[CrossRef](#)]
17. Pratt, W.P., Jr.; Lee, S.; Slaughter, J.M.; Loloee, R.; Schroeder, P.A.; Bass, J. Perpendicular giant magnetoresistances of Ag/Co multilayers. *Phys. Rev. Lett.* **1991**, *66*, 3060–3063. [[CrossRef](#)] [[PubMed](#)]
18. Valet, T.; Fert, A. Theory of the perpendicular magnetoresistance in magnetic multilayers. *Phys. Rev. B* **1993**, *48*, 7099. [[CrossRef](#)]
19. Coehoorn, R.; Gijs, M.A.M.; Grünberg, P.; Rasing, T.; Röhl, K.; van den Berg, H.A.M. *Magnetic Multilayers and Giant Magnetoresistance: Fundamentals and Industrial Applications*; Springer: Berlin, Germany, 2000; ISBN 978-3-662-04121-5.
20. Julliere, M. Tunneling between ferromagnetic films. *Phys. Lett. A* **1975**, *54*, 225–226. [[CrossRef](#)]
21. Miyazaki, T.; Tezuka, N. Giant magnetic tunneling effect in Fe/Al₂O₃/Fe junction. *J. Magn. Magn. Mater.* **1995**, *139*, L231–L234. [[CrossRef](#)]
22. Moodera, J.S.; Kinder, L.R.; Wong, T.M.; Meservey, R. Large magnetoresistance at room temperature in ferromagnetic thin film tunnel junctions. *Phys. Rev. Lett.* **1995**, *74*, 3273. [[CrossRef](#)] [[PubMed](#)]
23. Wei, H.; Qin, Q.; Ma, M.; Sharif, R.; Han, X. 80% tunneling magnetoresistance at room temperature for thin Al-O barrier magnetic tunnel junction with CoFeB as free and reference layers. *J. Appl. Phys.* **2007**, *101*, 09B501. [[CrossRef](#)]
24. Butler, W.H.; Zhang, X.; Schulthess, T.C.; MacLaren, J.M. Spin-dependent tunneling conductance of Fe|MgO|Fe sandwiches. *Phys. Rev. B* **2001**, *63*, 054416. [[CrossRef](#)]
25. Parkin, S.S.; Kaiser, C.; Panchula, A.; Rice, P.M.; Hughes, B.; Samant, M.; Yang, S. Giant tunnelling magnetoresistance at room temperature with MgO (100) tunnel barriers. *Nat. Mater.* **2004**, *3*, 862–867. [[CrossRef](#)] [[PubMed](#)]
26. Yuasa, S.; Nagahama, T.; Fukushima, A.; Suzuki, Y.; Ando, K. Giant room-temperature magnetoresistance in single-crystal Fe/MgO/Fe magnetic tunnel junctions. *Nat. Mater.* **2004**, *3*, 868–871. [[CrossRef](#)] [[PubMed](#)]

27. Lee, Y.M.; Hayakawa, J.; Ikeda, S.; Matsukura, F.; Ohno, H. Effect of electrode composition on the tunnel magnetoresistance of pseudo-spin-valve magnetic tunnel junction with a MgO tunnel barrier. *Appl. Phys. Lett.* **2007**, *90*, 212507. [[CrossRef](#)]
28. Ikeda, S.; Miura, K.; Yamamoto, H.; Mizunuma, K.; Gan, H.D.; Endo, M.; Kanai, S.; Hayakawa, J.; Matsukura, F.; Ohno, H. A perpendicular-anisotropy CoFeB-MgO magnetic tunnel junction. *Nat. Mater.* **2010**, *9*, 721–724. [[CrossRef](#)] [[PubMed](#)]
29. Dieny, B.; Chshiev, M. Perpendicular magnetic anisotropy at transition metal/oxide interfaces and applications. *Rev. Mod. Phys.* **2017**, *89*, 025008. [[CrossRef](#)]
30. Parkin, S.S. Origin of enhanced magnetoresistance of magnetic multilayers: Spin-dependent scattering from magnetic interface states. *Phys. Rev. Lett.* **1993**, *71*, 1641–1644. [[CrossRef](#)] [[PubMed](#)]
31. Camley, R.E.; Barnas, J. Theory of giant magnetoresistance effects in magnetic layered structures with antiferromagnetic coupling. *Phys. Rev. Lett.* **1989**, *63*, 664–667. [[CrossRef](#)] [[PubMed](#)]
32. Mott, N.F. The electrical conductivity of transition metals. *Proc. R. Soc. Lond. A* **1936**, *153*, 699–717. [[CrossRef](#)]
33. Fert, A.; Campbell, I.A. Two-current conduction in nickel. *Phys. Rev. Lett.* **1968**, *21*, 1190. [[CrossRef](#)]
34. Yuasa, S.; Djayaprawira, D.D. Giant tunnel magnetoresistance in magnetic tunnel junctions with a crystalline MgO (001) barrier. *J. Phys. D Appl. Phys.* **2007**, *40*, R337–R354. [[CrossRef](#)]
35. Hoffmann, A.; Bader, S.D. Opportunities at the Frontiers of Spintronics. *Phys. Rev. Appl.* **2015**, *4*, 047001. [[CrossRef](#)]
36. Wolf, S.A.; Awschalom, D.D.; Buhrman, R.A.; Daughton, J.M.; von Molnar, S.; Roukes, M.L.; Chtchelkanova, A.Y.; Treger, D.M. Spintronics: A spin-based electronics vision for the future. *Science* **2001**, *294*, 1488–1495. [[CrossRef](#)] [[PubMed](#)]
37. Fert, A.; Grünberg, P.; Barthélémy, A.; Petroff, F.; Zinn, W. Layered magnetic structures: Interlayer exchange coupling and giant magnetoresistance. *J. Magn. Magn. Mater.* **1995**, *140*, 1–8. [[CrossRef](#)]
38. Grünberg, P.; Schreiber, R.; Pang, Y.; Brodsky, M.B.; Sowers, H. Layered magnetic structures: Evidence for antiferromagnetic coupling of Fe layers across Cr interlayers. *Phys. Rev. Lett.* **1986**, *57*, 2442–2445. [[CrossRef](#)] [[PubMed](#)]
39. Carbone, C.; Alvarado, S.F. Antiparallel coupling between Fe layers separated by a Cr interlayer: Dependence of the magnetization on the film thickness. *Phys. Rev. B* **1987**, *36*, 2433–2435. [[CrossRef](#)]
40. Qiu, Z.Q.; Smith, N.V. Quantum well states and oscillatory magnetic interlayer coupling. *J. Phys. Condens. Mat.* **2002**, *14*, R169–R193. [[CrossRef](#)]
41. Parkin, S.S.P.; More, N.; Roche, K.P. Oscillations in exchange coupling and magnetoresistance in metallic superlattice structures: Co/Ru, Co/Cr, and Fe/Cr. *Phys. Rev. Lett.* **1990**, *64*, 2304–2307. [[CrossRef](#)] [[PubMed](#)]
42. Parkin, S.S.P.; Bhadra, R.; Roche, K.P. Oscillatory magnetic exchange coupling through thin copper layers. *Phys. Rev. Lett.* **1991**, *66*, 2152–2155. [[CrossRef](#)] [[PubMed](#)]
43. Parkin, S.S.P. Systematic variation of the strength and oscillation period of indirect magnetic exchange coupling through the 3d, 4d, and 5d transition metals. *Phys. Rev. Lett.* **1991**, *67*, 3598–3601. [[CrossRef](#)] [[PubMed](#)]
44. Mosca, D.H.; Petroff, F.; Fert, A.; Schroeder, P.A.; Pratt, W.P.; Laloe, R. Oscillatory interlayer coupling and giant magnetoresistance in Co/Cu multilayers. *J. Magn. Magn. Mater.* **1991**, *94*, L1–L5. [[CrossRef](#)]
45. Toscano, S.; Briner, B.; Hopster, H.; Landolt, M. Exchange-coupling between ferromagnets through a non-metallic amorphous spacer-layer. *J. Magn. Magn. Mater.* **1992**, *114*, L6–L10. [[CrossRef](#)]
46. Inomata, K.; Yusu, K.; Saito, Y. Magnetoresistance Associated with Antiferromagnetic Interlayer Coupling Spaced by a Semiconductor in Fe/Si Multilayers. *Phys. Rev. Lett.* **1995**, *74*, 1863–1866. [[CrossRef](#)] [[PubMed](#)]
47. Gareev, R.R.; Urgler, D.E.; Buchmeier, M.; Olligs, D.; Schreiber, R.; Grunberg, P. Metallic-Type Oscillatory Interlayer Exchange Coupling across an Epitaxial FeSi Spacer. *Phys. Rev. Lett.* **2001**, *87*, 157202. [[CrossRef](#)] [[PubMed](#)]
48. Chiba, D.; Akiba, N.; Matsukura, F.; Ohno, Y.; Ohno, H. Magnetoresistance effect and interlayer coupling of (Ga,Mn)As trilayer structures. *Appl. Phys. Lett.* **2000**, *77*, 1873–1875. [[CrossRef](#)]
49. Chung, J.H.; Chung, S.J.; Lee, S.; Kirby, B.J.; Borchers, J.A.; Cho, Y.J.; Liu, X.; Furdyna, J.K. Carrier-Mediated Antiferromagnetic Interlayer Exchange Coupling in Diluted Magnetic Semiconductor Multilayers Ga_{1-x}Mn_xAs/GaAs:Be. *Phys. Rev. Lett.* **2008**, *101*, 237202. [[CrossRef](#)] [[PubMed](#)]

50. Nistor, L.E.; Rodmacq, B.; Auffret, S.E.; Schuhl, A.; Chshiev, M.; Dieny, B. Oscillatory interlayer exchange coupling in MgO tunnel junctions with perpendicular magnetic anisotropy. *Phys. Rev. B* **2010**, *81*, 220407. [[CrossRef](#)]
51. Koziol-Rachwal, A.; Slezak, T.; Slezak, M.; Matlak, K.; Mlynczak, E.; Spiridis, N.; Korecki, J. Antiferromagnetic interlayer exchange coupling in epitaxial Fe/MgO/Fe trilayers with MgO barriers as thin as single monolayers. *J. Appl. Phys.* **2014**, *115*, 104301. [[CrossRef](#)]
52. Blouzon, C.; Ott, F.; Torteck, L.; Fichou, D.; Moussy, J.B. Anti-ferromagnetic coupling in hybrid magnetic tunnel junctions mediated by monomolecular layers of α -sexithiophene. *Appl. Phys. Lett.* **2013**, *103*, 042417. [[CrossRef](#)]
53. Fullerton, E.E.; Conover, M.J.; Mattson, J.E.; Sowers, C.H.; Bader, S.D. 150% magnetoresistance in sputtered Fe/Cr(100) superlattices. *Appl. Phys. Lett.* **1993**, *63*, 1699–1701. [[CrossRef](#)]
54. Bruno, P.; Chappert, C. Oscillatory coupling between ferromagnetic layers separated by a nonmagnetic metal spacer. *Phys. Rev. Lett.* **1991**, *67*, 1602–1605. [[CrossRef](#)] [[PubMed](#)]
55. Bruno, P. Theory of interlayer magnetic coupling. *Phys. Rev. B* **1995**, *52*, 411–439. [[CrossRef](#)]
56. Ortega, J.E.; Himpsel, F.J. Quantum well states as mediators of magnetic coupling in superlattices. *Phys. Rev. Lett.* **1992**, *69*, 844–847. [[CrossRef](#)] [[PubMed](#)]
57. Bürgler, D.E.; Grünberg, P.; Demokritov, S.O.; Johnson, M.T. Interlayer exchange coupling in layered magnetic structures. In *Handbook of Magnetic Materials*; Buschow, K.H.J., Ed.; Elsevier: Amsterdam, The Netherlands, 2001; Volume 13, pp. 1–85. ISBN 978-0-444-50666-5.
58. van Schilfgaarde, M.; Harrison, W.A. Oscillatory exchange coupling: RKKY or quantum-well mechanism? *Phys. Rev. Lett.* **1993**, *71*, 3870–3873. [[CrossRef](#)] [[PubMed](#)]
59. Zhu, J. Spin valve and dual spin valve heads with synthetic antiferromagnets. *IEEE Trans. Magn.* **1999**, *35*, 655–660. [[CrossRef](#)]
60. Parkin, S.S.P.; Mauri, D. Spin engineering: Direct determination of the Ruderman-Kittel-Kasuya-Yosida far-field range function in ruthenium. *Phys. Rev. B* **1991**, *44*, 7131–7134. [[CrossRef](#)]
61. Mattson, J.E.; Kumar, S.; Fullerton, E.E.; Lee, S.R.; Sowers, C.H.; Grimsditch, M.; Bader, S.D.; Parker, F.T. Photoinduced antiferromagnetic interlayer coupling in Fe/(Fe-Si) superlattices. *Phys. Rev. Lett.* **1993**, *71*, 185–188. [[CrossRef](#)] [[PubMed](#)]
62. Briner, B.; Landolt, M. Intrinsic and Heat-Induced Exchange Coupling through Amorphous Silicon. *Phys. Rev. Lett.* **1994**, *73*, 340–343. [[CrossRef](#)] [[PubMed](#)]
63. Hunziker, M.; Landolt, M. Heat-induced effective exchange in magnetic multilayers. *Phys. Rev. B* **2001**, *64*, 134421. [[CrossRef](#)]
64. Ueda, S.; Iwasaki, Y.; Uehara, Y.; Ushioda, S. Changes of interlayer exchange coupling in Fe/Si/Fe trilayer structure by photo-irradiation. *Phys. Rev. B* **2011**, *83*, 144424. [[CrossRef](#)]
65. Tang, Z.; Sun, F.; Han, B.; Yu, K.; Zhu, Z.; Chu, J. Tuning Interlayer Exchange Coupling of Co-Doped TiO₂/VO₂ Multilayers via Metal-Insulator Transition. *Phys. Rev. Lett.* **2013**, *111*, 107203. [[CrossRef](#)] [[PubMed](#)]
66. Meng, H.; Wang, J.; Diao, Z.; Wang, J. Low resistance spin-dependent magnetic tunnel junction with high breakdown voltage for current-induced-magnetization-switching devices. *J. Appl. Phys.* **2005**, *97*, 10C926. [[CrossRef](#)]
67. Sukegawa, H.; Xiu, H.; Ohkubo, T.; Furubayashi, T.; Niizeki, T.; Wang, W.; Kasai, S.; Mitani, S.; Inomata, K.; Hono, K. Tunnel magnetoresistance with improved bias voltage dependence in lattice-matched Fe/spinel MgAl₂O₄/Fe(001) junctions. *Appl. Phys. Lett.* **2010**, *96*, 212505. [[CrossRef](#)]
68. Zhang, J.; Zhang, X.; Han, X. Spinel oxides: Δ_1 spin-filter barrier for a class of magnetic tunnel junctions. *Appl. Phys. Lett.* **2012**, *100*, 222401. [[CrossRef](#)]
69. Zhou, J.; Zhao, W.; Wang, Y.; Peng, S.; Qiao, J.; Su, L.; Zeng, L.; Lei, N.; Liu, L.; Zhang, Y.; et al. Large influence of capping layers on tunnel magnetoresistance in magnetic tunnel junctions. *Appl. Phys. Lett.* **2016**, *109*, 242403. [[CrossRef](#)]
70. Zhang, B.; Cao, A.; Qiao, J.; Tang, M.; Cao, K.; Zhao, X.; Eimer, S.; Si, Z.; Lei, N.; Wang, Z.; et al. Influence of heavy metal materials on magnetic properties of Pt/Co/heavy metal tri-layered structures. *Appl. Phys. Lett.* **2017**, *110*, 012405. [[CrossRef](#)]
71. Rizal, C.; Fullerton, E.E. Perpendicular magnetic anisotropy and microstructure properties of nanoscale Co/Au multilayers. *J. Phys. D Appl. Phys.* **2017**, *50*, 355002. [[CrossRef](#)]

72. Appelbaum, I.; Huang, B.; Monsma, D.J. Electronic measurement and control of spin transport in silicon. *Nature* **2007**, *447*, 295–298. [[CrossRef](#)] [[PubMed](#)]
73. Tanaka, M.; Higo, Y. Large Tunneling Magnetoresistance in GaMnAs/AlAs/GaMnAs Ferromagnetic Semiconductor Tunnel Junctions. *Phys. Rev. Lett.* **2001**, *87*, 026602. [[CrossRef](#)]
74. Saito, H.; Yuasa, S.; Ando, K. Origin of the tunnel anisotropic magnetoresistance in Ga_{1-x}Mn_xAs/ZnSe/Ga_{1-x}Mn_xAs magnetic tunnel junctions of II-VI/III-V heterostructures. *Phys. Rev. Lett.* **2005**, *95*, 086604. [[CrossRef](#)] [[PubMed](#)]
75. Schmidt, G.; Ferrand, D.; Molenkamp, L.W.; Filip, A.T.; van Wees, B.J. Fundamental obstacle for electrical spin injection from a ferromagnetic metal into a diffusive semiconductor. *Phys. Rev. B* **2000**, *62*, R4790–R4793. [[CrossRef](#)]
76. Awschalom, D.D.; Flatte, M.E. Challenges for semiconductor spintronics. *Nat. Phys.* **2007**, *3*, 153–159. [[CrossRef](#)]
77. Kienberger, R.; Goulielmakis, E.; Uiberacker, M.; Baltuska, A.; Yakovlev, V.; Bammer, F.; Scrinzi, A.; Westerwalbesloh, T.; Kleineberg, U.; Heinzmann, U.; et al. Atomic transient recorder. *Nature* **2004**, *427*, 817–821. [[CrossRef](#)] [[PubMed](#)]
78. Naber, W.J.M.; Faez, S.; van der Wiel, W.G. Organic spintronics. *J. Phys. D Appl. Phys.* **2007**, *40*, R205–R228. [[CrossRef](#)]
79. Geng, R.; Daugherty, T.T.; Do, K.; Luong, H.M.; Nguyen, T.D. A review on organic spintronic materials and devices: I. Magnetic field effect on organic light emitting diodes. *J. Sci. Adv. Mater. Devices* **2016**, *1*, 128–140. [[CrossRef](#)]
80. Geng, R.; Luong, H.M.; Daugherty, T.T.; Hornak, L.; Nguyen, T.D. A review on organic spintronic materials and devices: II. Magnetoresistance in organic spin valves and spin organic light emitting diodes. *J. Sci. Adv. Mater. Devices* **2016**, *1*, 256–272. [[CrossRef](#)]
81. Tsukagoshi, K.; Alphenaar, B.W.; Ago, H. Coherent transport of electron spin in a ferromagnetically contacted carbon nanotube. *Nature* **1999**, *401*, 572–574. [[CrossRef](#)]
82. Hueso, L.E.; Pruneda, J.M.; Ferrari, V.; Burnell, G.; Valdes-Herrera, J.P.; Simons, B.D.; Littlewood, P.B.; Artacho, E.; Fert, A.; Mathur, N.D. Transformation of spin information into large electrical signals using carbon nanotubes. *Nature* **2007**, *445*, 410–413. [[CrossRef](#)] [[PubMed](#)]
83. Dediu, V.A.; Hueso, L.E.; Bergenti, I.; Taliani, C. Spin routes in organic semiconductors. *Nat. Mater.* **2009**, *8*, 850. [[CrossRef](#)]
84. Xiong, Z.; Wu, D.; Vardeny, Z.V.; Shi, J. Giant magnetoresistance in organic spin-valves. *Nature* **2004**, *427*, 821–824. [[CrossRef](#)] [[PubMed](#)]
85. Sun, D.; Yin, L.; Sun, C.; Guo, H.; Gai, Z.; Zhang, X.; Ward, T.Z.; Cheng, Z.; Shen, J. Giant Magnetoresistance in Organic Spin Valves. *Phys. Rev. Lett.* **2010**, *104*, 236602. [[CrossRef](#)] [[PubMed](#)]
86. Barraud, C.E.; Bouzehouane, K.; Deranlot, C.; Fusil, S.E.; Jabbar, H.; Arabski, J.; Rakshit, R.; Kim, D.; Kieber, C.; Boukari, S.; et al. Unidirectional Spin-Dependent Molecule-Ferromagnet Hybridized States Anisotropy in Cobalt Phthalocyanine Based Magnetic Tunnel Junctions. *Phys. Rev. Lett.* **2015**, *114*, 206603. [[CrossRef](#)] [[PubMed](#)]
87. Sun, X.; Bedoya-Pinto, A.; Mao, Z.; Gobbi, M.; Yan, W.; Guo, Y.; Atxabal, A.; Llopis, R.; Yu, G.; Liu, Y.; et al. Active Morphology Control for Concomitant Long Distance Spin Transport and Photoresponse in a Single Organic Device. *Adv. Mater.* **2016**, *28*, 2609–2615. [[CrossRef](#)] [[PubMed](#)]
88. Sun, X.; Velez, S.; Atxabal, A.; Bedoya-Pinto, A.; Parui, S.; Zhu, X.; Llopis, R.; Casanova, F.; Hueso, L.E. A molecular spin-photovoltaic device. *Science* **2017**, *357*, 677–680. [[CrossRef](#)] [[PubMed](#)]
89. López-Encarnación, J.M.; Burton, J.D.; Tsymbal, E.Y.; Velez, J.P. Organic Multiferroic Tunnel Junctions with Ferroelectric Poly(vinylidene fluoride) Barriers. *Nano Lett.* **2011**, *11*, 599–603. [[CrossRef](#)] [[PubMed](#)]
90. Liang, S.; Yang, H.; Yang, H.; Tao, B.; Djeflal, A.; Chshiev, M.; Huang, W.; Li, X.; Ferri, A.; Desfeux, R.; et al. Ferroelectric Control of Organic/Ferromagnetic Spininterface. *Adv. Mater.* **2016**, *28*, 10204–10210. [[CrossRef](#)] [[PubMed](#)]
91. Bowen, M.; Bibes, M.; Barthélémy, A.; Contour, J.P.; Anane, A.; Lemaître, Y.; Fert, A. Nearly total spin polarization in La_{2/3}Sr_{1/3}MnO₃ from tunneling experiments. *Appl. Phys. Lett.* **2003**, *82*, 233–235. [[CrossRef](#)]
92. Palmstrøm, C.J. Heusler compounds and spintronics. *Prog. Cryst. Growth Charact.* **2016**, *62*, 371–397. [[CrossRef](#)]

93. Esquinazi, P.; Hergert, W.; Spemann, D.; Setzer, A.; Ernst, A. Defect-Induced Magnetism in Solids. *IEEE Trans. Magn.* **2013**, *49*, 4668–4674. [[CrossRef](#)]
94. Botsch, L.; Lorite, I.; Kumar, Y.; Esquinazi, P.; Michalsky, T.; Zajadacz, J.; Zimmer, K. Spin-filter effect at the interface of magnetic/non-magnetic homojunctions in Li doped ZnO nanostructures. *arXiv*, 2017.
95. Stanciu, C.D.; Hansteen, F.; Kimel, A.V.; Kirilyuk, A.; Tsukamoto, A.; Itoh, A.; Rasing, T. All-optical magnetic recording with circularly polarized light. *Phys. Rev. Lett.* **2007**, *99*, 047601. [[CrossRef](#)] [[PubMed](#)]
96. Mangin, S.; Gottwald, M.; Lambert, C.; Steil, D.; Uhlř, V.; Pang, L.; Hehn, M.; Alebrand, S.; Cinchetti, M.; Malinowski, G.; et al. Engineered materials for all-optical helicity-dependent magnetic switching. *Nat. Mater.* **2014**, *13*, 286–292. [[CrossRef](#)] [[PubMed](#)]
97. Lorite, I.; Kumar, Y.; Esquinazi, P.; Friedländer, S.; Pöppel, A.; Michalsky, T.; Meijer, J.; Grundmann, M.; Meyer, T.; Estrela-Lopis, I. Photo-enhanced magnetization in Fe-doped ZnO nanowires. *Appl. Phys. Lett.* **2016**, *109*, 012401. [[CrossRef](#)]
98. Eerenstein, W.; Mathur, N.D.; Scott, J.F. Multiferroic and magnetoelectric materials. *Nature* **2006**, *442*, 759–765. [[CrossRef](#)] [[PubMed](#)]
99. Weisheit, M.; Faehler, S.; Marty, A.; Souche, Y.; Poinignon, C.; Givord, D. Electric field-induced modification of magnetism in thin-film ferromagnets. *Science* **2007**, *315*, 349–351. [[CrossRef](#)] [[PubMed](#)]
100. Koch, R.H.; Grinstein, G.; Keefe, G.A.; Lu, Y.; Trouilloud, P.L.; Gallagher, W.J.; Parkin, S.S.P. Thermally Assisted Magnetization Reversal in Submicron-Sized Magnetic Thin Films. *Phys. Rev. Lett.* **2000**, *84*, 5419–5422. [[CrossRef](#)] [[PubMed](#)]
101. Zutic, I.; Fabian, J.; Das Sarma, S. Spintronics: Fundamentals and applications. *Rev. Mod. Phys.* **2004**, *76*, 323–410. [[CrossRef](#)]
102. Slonczewski, J.C. Current-driven excitation of magnetic multilayers. *J. Magn. Magn. Mater.* **1996**, *159*, L1–L7. [[CrossRef](#)]
103. Katine, J.A.; Albert, F.J.; Buhrman, R.A.; Myers, E.B.; Ralph, D.C. Current-driven magnetization reversal and spin-wave excitations in Co/Cu/Co pillars. *Phys. Rev. Lett.* **2000**, *84*, 3149–3152. [[CrossRef](#)] [[PubMed](#)]
104. Kubota, H.; Fukushima, A.; Yakushiji, K.; Nagahama, T.; Yuasa, S.; Ando, K.; Maehara, H.; Nagamine, Y.; Tsunekawa, K.; Djayaprawira, D.D.; et al. Quantitative measurement of voltage dependence of spin-transfer torque in MgO-based magnetic tunnel junctions. *Nat. Phys.* **2008**, *4*, 37–41. [[CrossRef](#)]
105. Manchon, A.; Zhang, S. Theory of spin torque due to spin-orbit coupling. *Phys. Rev. B* **2009**, *79*, 094422. [[CrossRef](#)]
106. Liu, L.; Pai, C.; Li, Y.; Tseng, H.W.; Ralph, D.C.; Buhrman, R.A. Spin-Torque Switching with the Giant Spin Hall Effect of Tantalum. *Science* **2012**, *336*, 555–558. [[CrossRef](#)] [[PubMed](#)]
107. Yu, G.; Upadhyaya, P.; Fan, Y.; Alzate, J.G.; Jiang, W.; Wong, K.L.; Takei, S.; Bender, S.A.; Chang, L.; Jiang, Y.; et al. Switching of perpendicular magnetization by spin-orbit torques in the absence of external magnetic fields. *Nat. Nanotechnol.* **2014**, *9*, 548–554. [[CrossRef](#)] [[PubMed](#)]
108. Wang, W.; Li, M.; Hageman, S.; Chien, C.L. Electric-field-assisted switching in magnetic tunnel junctions. *Nat. Mater.* **2012**, *11*, 64–68. [[CrossRef](#)] [[PubMed](#)]
109. Li, Z.; Zhang, S. Thermally assisted magnetization reversal in the presence of a spin-transfer torque. *Phys. Rev. B* **2004**, *69*, 134416. [[CrossRef](#)]
110. Pushp, A.; Phung, T.; Rettner, C.; Hughes, B.P.; Yang, S.; Parkin, S.S.P. Giant thermal spin-torque-assisted magnetic tunnel junction switching. *Proc. Natl. Acad. Sci. USA* **2015**, *112*, 6585–6590. [[CrossRef](#)] [[PubMed](#)]
111. Lei, N.; Devolder, T.; Agnus, G.; Aubert, P.; Daniel, L.; Kim, J.; Zhao, W.; Trypiniotis, T.; Cowburn, R.P.; Chappert, C.; et al. Strain-controlled magnetic domain wall propagation in hybrid piezoelectric/ferromagnetic structures. *Nat. Commun.* **2013**, *4*, 1378. [[CrossRef](#)] [[PubMed](#)]
112. Chen, J.; He, L.; Wang, J.; Li, M. All-Optical Switching of Magnetic Tunnel Junctions with Single Subpicosecond Laser Pulses. *Phys. Rev. Appl.* **2017**, *7*, 021001. [[CrossRef](#)]
113. Desai, P.; Shakya, P.; Kreouzis, T.; Gillin, W.P. Magnetoresistance in organic light-emitting diode structures under illumination. *Phys. Rev. B* **2007**, *76*, 235202. [[CrossRef](#)]
114. Yuldashev, S.U.; Shon, Y.; Kwon, Y.H.; Fu, D.J.; Kim, D.Y.; Kim, H.J.; Kang, T.W.; Fan, X. Enhanced positive magnetoresistance effect in GaAs with nanoscale magnetic clusters. *J. Appl. Phys.* **2001**, *90*, 3004–3006. [[CrossRef](#)]
115. Kryder, M.H.; Gage, E.C.; Mcdaniel, T.W.; Challener, W.A.; Rottmayer, R.E.; Ju, G.; Hsia, Y.; Erden, M.F. Heat Assisted Magnetic Recording. *Proc. IEEE* **2008**, *96*, 1810–1835. [[CrossRef](#)]

116. Kimel, A.V.; Kirilyuk, A.; Usachev, P.A.; Pisarev, R.V.; Balbashov, A.M.; Rasing, T. Ultrafast non-thermal control of magnetization by instantaneous photomagnetic pulses. *Nature* **2005**, *435*, 655–657. [[CrossRef](#)] [[PubMed](#)]
117. Lambert, C.H.; Mangin, S.; Varaprasad, B.S.; Takahashi, Y.K.; Hehn, M.; Cinchetti, M.; Malinowski, G.; Hono, K.; Fainman, Y.; Aeschlimann, M.; et al. All-optical control of ferromagnetic thin films and nanostructures. *Science* **2014**, *345*, 1337–1340. [[CrossRef](#)] [[PubMed](#)]
118. Stupakiewicz, A.; Szerenos, K.; Afanasiev, D.; Kirilyuk, A.; Kimel, A.V. Ultrafast nonthermal photo-magnetic recording in a transparent medium. *Nature* **2017**, *542*, 71–74. [[CrossRef](#)] [[PubMed](#)]
119. Ostler, T.A.; Barker, J.; Evans, R.F.L.; Chantrell, R.W.; Atxitia, U.; Chubykalo-Fesenko, O.; El Moussaoui, S.; Le Guyader, L.; Mengotti, E.; Heyderman, L.J.; et al. Ultrafast heating as a sufficient stimulus for magnetization reversal in a ferrimagnet. *Nat. Commun.* **2012**, *3*, 666. [[CrossRef](#)] [[PubMed](#)]
120. Radu, I.; Vahaplar, K.; Stamm, C.; Kachel, T.; Pontius, N.; Duerr, H.A.; Ostler, T.A.; Barker, J.; Evans, R.F.L.; Chantrell, R.W.; et al. Transient ferromagnetic-like state mediating ultrafast reversal of antiferromagnetically coupled spins. *Nature* **2011**, *472*, 205–208. [[CrossRef](#)] [[PubMed](#)]
121. Xu, Y.; Deb, M.; Malinowski, G.; Hehn, M.; Zhao, W.; Mangin, S. Ultrafast Magnetization Manipulation Using Single Femtosecond Light and Hot-Electron Pulses. *Adv. Mater.* **2017**, *29*, 1703474. [[CrossRef](#)] [[PubMed](#)]
122. Wilson, R.B.; Gorchon, J.; Yang, Y.; Lambert, C.; Salahuddin, S.; Bokor, J. Ultrafast magnetic switching of GdFeCo with electronic heat currents. *Phys. Rev. B* **2017**, *95*, 180409. [[CrossRef](#)]
123. El Hadri, M.S.; Hehn, M.; Pirro, P.; Lambert, C.; Malinowski, G.; Fullerton, E.E.; Mangin, S. Domain size criterion for the observation of all-optical helicity-dependent switching in magnetic thin films. *Phys. Rev. B* **2016**, *94*, 064419. [[CrossRef](#)]
124. Choi, G.; Schleife, A.; Cahill, D.G. Optical-helicity-driven magnetization dynamics in metallic ferromagnets. *Nat. Commun.* **2017**, *8*, 15085. [[CrossRef](#)] [[PubMed](#)]
125. Gorchon, J.; Yang, Y.; Bokor, J. Model for multishot all-thermal all-optical switching in ferromagnets. *Phys. Rev. B* **2016**, *94*, 0204092. [[CrossRef](#)]
126. Berritta, M.; Mondal, R.; Carva, K.; Oppeneer, P.M. Ab Initio Theory of Coherent Laser-Induced Magnetization in Metals. *Phys. Rev. Lett.* **2016**, *117*, 137203. [[CrossRef](#)] [[PubMed](#)]
127. Yang, Y.; Wilson, R.B.; Gorchon, J.; Lambert, C.H.; Salahuddin, S.; Bokor, J. Ultrafast magnetization reversal by picosecond electrical pulses. *Sci. Adv.* **2017**, *3*, e1603117. [[CrossRef](#)] [[PubMed](#)]
128. Mattson, J.E.; Fullerton, E.E.; Kumar, S.; Lee, S.R.; Sowers, C.H.; Grimsditch, M.; Bader, S.D.; Parker, F.T. Photo-induced antiferromagnetic interlayer coupling in Fe superlattices with iron silicide spacers (invited). *J. Appl. Phys.* **1994**, *75*, 6169–6173. [[CrossRef](#)]
129. Grollier, J.; Querlioz, D.; Stiles, M.D. Spintronic Nanodevices for Bioinspired Computing. *Proc. IEEE* **2016**, *104*, 2024–2039. [[CrossRef](#)] [[PubMed](#)]
130. Xiao, G. Magnetoresistive Sensors Based on Magnetic Tunneling Junctions. In *Handbook of Spin Transport and Magnetism*; Tsymbal, E., Zutic, I., Eds.; CRC Press: Boca Raton, FL, USA, 2012; ISBN 9781439803776.
131. Rieger, G.; Ludwig, K.; Hauch, J.; Clemens, W. GMR sensors for contactless position detection. *Sens. Actuators A Phys.* **2001**, *91*, 7–11. [[CrossRef](#)]
132. Giebler, C.; Adelerhof, D.J.; Kuiper, A.E.T.; van Zon, J.B.A.; Oelgeschläger, D.; Schulz, G. Robust GMR sensors for angle detection and rotation speed sensing. *Sens. Actuators A Phys.* **2001**, *91*, 16–20. [[CrossRef](#)]
133. Freitas, P.P.; Ferreira, R.; Cardoso, S. Spintronic Sensors. *Proc. IEEE* **2016**, *104*, 1894–1918. [[CrossRef](#)]
134. De Boer, B.M.; Kahlman, J.A.H.M.; Jansen, T.P.G.H.; Duric, H.; Veen, J. An integrated and sensitive detection platform for magneto-resistive biosensors. *Biosens. Bioelectron.* **2007**, *22*, 2366–2370. [[CrossRef](#)] [[PubMed](#)]
135. Hall, D.A.; Gaster, R.S.; Lin, T.; Osterfeld, S.J.; Han, S.; Murmann, B.; Wang, S.X. GMR biosensor arrays: A system perspective. *Biosens. Bioelectron.* **2010**, *25*, 2051–2057. [[CrossRef](#)] [[PubMed](#)]
136. Rizal, C.; Niraula, B.; Lee, H. Bio-Magnetoplasmonics, Emerging Biomedical Technologies and Beyond. *J. Nanomed. Res.* **2016**, *3*, 00059. [[CrossRef](#)]
137. Schrag, B.D.; Liu, X.; Shen, W.; Xiao, G. Current density mapping and pinhole imaging in magnetic tunnel junctions via scanning magnetic microscopy. *Appl. Phys. Lett.* **2004**, *84*, 2937–2939. [[CrossRef](#)]
138. Kent, A.D.; Worledge, D.C. A new spin on magnetic memories. *Nat. Nanotechnol.* **2015**, *10*, 187–191. [[CrossRef](#)] [[PubMed](#)]
139. Zhu, J. Magnetoresistive Random Access Memory: The Path to Competitiveness and Scalability. *Proc. IEEE* **2008**, *96*, 1786–1798. [[CrossRef](#)]

140. Apalkov, D.; Dieny, B.; Slaughter, J.M. Magnetoresistive Random Access Memory. *Proc. IEEE* **2016**, *104*, 1796–1830. [[CrossRef](#)]
141. Parkin, S.; Yang, S. Memory on the racetrack. *Nat. Nanotechnol.* **2015**, *10*, 195–198. [[CrossRef](#)] [[PubMed](#)]
142. Kang, W.; Huang, Y.; Zhang, X.; Zhou, Y.; Zhao, W. Skyrmion-Electronics: An Overview and Outlook. *Proc. IEEE* **2016**, *104*, 2040–2061. [[CrossRef](#)]
143. Lin, X.; Su, L.; Si, Z.; Zhang, Y.; Bournel, A.; Zhang, Y.; Klein, J.; Fert, A.; Zhao, W. Gate-Driven Pure Spin Current in Graphene. *Phys. Rev. Appl.* **2017**, *8*, 034006. [[CrossRef](#)]
144. Chumak, A.V.; Vasyuchka, V.I.; Serga, A.A.; Hillebrands, B. Magnon spintronics. *Nat. Phys.* **2015**, *11*, 453–461. [[CrossRef](#)]
145. Savoini, M.; Medapalli, R.; Koene, B.; Khorsand, A.R.; Le Guyader, L.; Duo, L.; Finazzi, M.; Tsukamoto, A.; Itoh, A.; Nolting, F.; et al. Highly efficient all-optical switching of magnetization in GdFeCo microstructures by interference-enhanced absorption of light. *Phys. Rev. B* **2012**, *86*, 140404. [[CrossRef](#)]



© 2017 by the authors. Licensee MDPI, Basel, Switzerland. This article is an open access article distributed under the terms and conditions of the Creative Commons Attribution (CC BY) license (<http://creativecommons.org/licenses/by/4.0/>).